AGU PUBLICATIONS

JGR

Journal of Geophysical Research: Space Physics

RESEARCH ARTICLE
10.1002/2014JA020151

Key Points:
- Impulsive energy at CME front causes severe space weather (SvSW) in heliosphere
- Impulsive energy and IMF Bz southward at the CME front causes SvSW at the Earth
- Northward IMF Bz at the CME front causes normal space weather at the Earth

Correspondence to:
N. Balan,
b.nanan@sheffield.ac.uk

Citation:
Balan, N., R. Skoug, S. Tulasi Ram, P. K. Rajesh, K. Shiokawa, Y. Otsuka, I. S. Batista, Y. Ebihara, and T. Nakamura (2014), CME front and severe space weather, *J. Geophys. Res. Space Physics*, *119*, doi:10.1002/2014JA020151.

Received 4 MAY 2014
Accepted 22 NOV 2014
Accepted article online 26 NOV 2014

CME front and severe space weather

N. Balan[1,2,3], R. Skoug[4], S. Tulasi Ram[5], P. K. Rajesh[2], K. Shiokawa[1], Y. Otsuka[1], I. S. Batista[6], Y. Ebihara[3], and T. Nakamura[7]

[1]Solar Terrestrial Environment Laboratory, Nagoya University, Nagoya, Japan, [2]Department of Physics, National Cheng Kung University, Tainan, Taiwan, [3]RISH, Kyoto University, Uji, Kyoto, Japan, [4]Los Alamos National Laboratory, Los Alamos, New Mexico, USA, [5]Indian Institute of Geomagnetism, Navi Mumbai, India, [6]INPE, São Paulo, Brazil, [7]NIPR, Tachikawa, Tokyo, Japan

Abstract Thanks to the work of a number of scientists who made it known that severe space weather can cause extensive social and economic disruptions in the modern high-technology society. It is therefore important to understand what determines the severity of space weather and whether it can be predicted. We present results obtained from the analysis of coronal mass ejections (CMEs), solar energetic particle (SEP) events, interplanetary magnetic field (IMF), CME-magnetosphere coupling, and geomagnetic storms associated with the major space weather events since 1998 by combining data from the ACE and GOES satellites with geomagnetic parameters and the Carrington event of 1859, the Quebec event of 1989, and an event in 1958. The results seem to indicate that (1) it is the impulsive energy mainly due to the impulsive velocity and orientation of IMF B_z at the leading edge of the CMEs (or CME front) that determine the severity of space weather. (2) CMEs having high impulsive velocity (sudden nonfluctuating increase by over 275 km s^{-1} over the background) caused severe space weather (SvSW) in the heliosphere (failure of the solar wind ion mode of Solar Wind Electron Proton Alpha Monitor in ACE) probably by suddenly accelerating the high-energy particles in the SEPs ahead directly or through the shocks. (3) The impact of such CMEs which also show the IMF B_z southward from the leading edge caused SvSW at the Earth including extreme geomagnetic storms of mean $Dst_{MP} < -250$ nT during main phases, and the known electric power outages happened during some of these SvSW events. (4) The higher the impulsive velocity, the more severe the space weather, like faster weather fronts and tsunami fronts causing more severe damage through impulsive action. (5) The CMEs having IMF B_z northward at the leading edge do not seem to cause SvSW on Earth, although, later when the IMF B_z turns southward, they can lead to super geomagnetic storms of intensity (Dst_{min}) less than even -400 nT.

1. Introduction

Like Earth, the Sun has (11 year) climate and many types of weather. The solar weather escaping from the solar gravitational pull (escape velocity = 617.5 km/s) includes coronal mass ejections or CMEs [e.g., *MacQueen et al.*, 1974]. CMEs flow out through the interplanetary space (as ICMEs or interplanetary CMEs) with high speeds up to thousands of kilometers per second compared to typical solar wind speed of ~400 km s^{-1}, high densities up to 100/cm^3 compared to normal solar wind density of <5/cm^3, and strong magnetic fields up to 100 nT compared to normal interplanetary magnetic field (IMF) of <5 nT [e.g., *Skoug et al.*, 2004; *Gopalswamy et al.*, 2005a]. While flowing out, the CMEs and ICMEs cause rapid and sometimes severe changes in the heliosphere [e.g., *Manoharan*, 2006] and in the environment of the planets. These changes are known as space weather.

Solar energetic particle (SEP) events are highly energetic up to 100 MeV and are part of space weather. Before 1990, as their name implies, SEPs were believed to be driven mostly by solar flares. Later, based on observational results, it was realized that large SEP events are driven by CME shock waves rather than by solar flares [e.g., *Cliver et al.*, 1990; *Reames et al.*, 1996; *Kahler and Vourlidas*, 2005; *Marusek*, 2007; *Singh et al.*, 2010]. The highest-energy particles can even penetrate the skin of space probes and damage spacecraft subsystems and payload instrumentation [e.g., *McKenna-Lawlor*, 2008]. Communications with spacecraft can also be affected due to plasma-induced surface charging and energetic charged particle-induced internal charging.

The space weather in Earth's environment generally includes (1) sudden compression of the magnetosphere [e.g., *Russell et al.*, 1999; *Balan et al.*, 2008]; (2) intensification of ring currents and the occurrence of geomagnetic

storms and auroras [e.g., *Gonzalez et al.*, 1994; *Kamide et al.*, 1998a, 1998b; *Ebihara et al.*, 2005]; (3) changes in ionospheric electric fields and currents [e.g., *Rastogi*, 1977; *Kikuchi et al.*, 1978; *Kelley et al.*, 2003; *Huang et al.*, 2010; *Tulasi Ram et al.*, 2012]; (4) heating and expansion of the high-latitude upper atmosphere, which generates thermospheric storms [e.g., *Mayr and Volland*, 1973; *Fuller-Rowell et al.*, 1994; *Tulasi Ram et al.*, 2010]; and (5) changes in ionospheric density and temperature, which are known as ionospheric storms [e.g., *Matuura*, 1972; *Lin et al.*, 2005; *Heelis et al.*, 2009; *Balan et al.*, 2010; *Lu et al.*, 2012; *Sojka et al.*, 2012].

Like Earth's weather, space weather occasionally becomes severe [e.g., *Baker et al.*, 2013]. When it becomes severe, it can cause extensive social and economic disruptions in the modern high-technology society [e.g., *Baker*, 2002; *Pulkkinen*, 2007; *Hapgood*, 2011] by damaging (a) satellite systems [e.g., *Barbieri and Mahmot*, 2004], (b) electric power grids [e.g., *Kappenman*, 1996], (c) oil and gas metal pipe line systems [e.g., *Viljanen et al.*, 2006], (d) long-distance communication cables [e.g., *Medford et al.*, 1989], (e) satellite communication and navigation [e.g., *Lanzerotti*, 2001], (f) ground-based communication [e.g., *Prolss*, 1995], etc.

The most famous space weather event known as the Carrington event happened in September 1859 [e.g., *Carrington*, 1859]. The famous electric power outage in Quebec happened during the space weather event on 13 March 1989 [e.g., *Medford et al.*, 1989; *Bolduc*, 2002; *Batista et al.*, 1991]. The November 2001 event and the Halloween 2003 event caused satellite system failures [e.g., *Skoug et al.*, 2004; *Webb and Allen*, 2004; *Terasawa et al.*, 2005], electric power outages [e.g., *Pulkkinen et al.*, 2005; *Wik et al.*, 2009; *Marshall et al.*, 2012], and produced extreme geomagnetic storms. The events also caused other extreme space weather effects [e.g., *Mannucci et al.*, 2005; *Batista et al.*, 2006; *Abdu et al.*, 2008; *Balan et al.*, 2011, and references therein]. *Gopalswamy et al.* [2005b] edited a special issue of Geophysical Research Letters on the space weather effects observed during the Halloween 2003 period. Excellent review articles on different aspects of space weather have been presented, for example, by *Barbieri and Mahmot* [2004], *Schwenn* [2006], *Pulkkinen* [2007], and *Shibata and Magara* [2011].

It has been estimated that an event such as the Carrington event at present times would cause very serious social and economic disturbances [e.g., *Baker*, 2002; *Pulkkinen*, 2007]. It is therefore important to understand and predict the occurrence of severe space weather (SvSW). In a probability study using solar flare intensity, CME speed, *Dst* index, and >30 MeV proton fluxes, *Riley* [2012] predicts a probability of 12% for a Carrington-type event ($Dst < -850$ nT) to occur within the next decade. Based on nitrate measurements from ice core samples [*Shea et al.*, 2006], *Barnard et al.* [2011] inferred a probability of occurrence of 2.6 per century for major SEP events. Observations and modeling of solar flares [e.g., *Benz*, 2008; *Shibata and Magara*, 2011] and analysis of geomagnetic storms [e.g., *Tsurutani et al.*, 2003; *Cliver and Svalgaard*, 2004] suggest that events as severe as or more severe than the Carrington event can occur again. Indeed, a similar event occurred in July 2012 though was not Earth directed [e.g., *Baker et al.*, 2013; *Russell et al.*, 2013].

Although tremendous progress has been made, what determines the severity of space weather is not yet understood. We present results obtained from the analysis of solar-geophysical data (section 2) since 1998 when continuous measurements of solar wind, IMF, and SEP data are available [e.g., *McComas et al.*, 1998; *Skoug et al.*, 2004] and the Carrington event of September 1859, the Quebec event of March 1989, and another possible severe event in February 1958. Following a definition of severe space weather (SvSW) in section 3, the results are presented in section 4, which indicate that it is the characteristics at the leading edge of the CMEs (or CME front) that determine the severity of space weather. The results are discussed in section 5, which includes a prediction scheme.

2. Data and Analysis

The solar wind and IMF data measured by the ACE (Advanced Composition Explorer) satellite since 1998 and available at California Institute of Technology (http://www.srl.caltech.edu/ACE/ASC/), >30 MeV SEP flux measured by the GOES 10 satellite and available at 5 min resolution and time corrected to bow shock nose at http://cdaweb.gsfc.nasa.gov/cgi-bin/eval2.cgi(OMNI_HRO_5MIN), and geomagnetic activity (*Dst* and *AE*) data available at the Kyoto World Data Center (http://wdc.kugi.kyoto-u.ac.jp/dstdir/) form the main data sources. The IMP 8 (Interplanetary Monitoring Platform) solar wind data available at

Table 1. Characteristics of the Geomagnetic Storms Associated With 13 Major Space Weather Events Since 1998 and the Carrington Event of September 1959, the Quebec Event of March 1989, and an Event in February 1958[a]

	Main Phase Onset									
Storm No.	D	M	Y	Dst_{min} (nT)	MP (h)	Duration (UT)	Mean Dst_{MP} (nT)	$(\delta Dst/\delta t)_{MPmax}$ (nT)	AE_{max} (nT)	Mean AE_{MP} (nT)
1	**1/9/1859**			**1710**	**2**	**04–06**	**700**	**1390**	**no data**	
2	*29/10/2003*			*−353*	*18 F*	*07–01*	*−179*	*95*	*2241*	*1307*
3	**13/3/1989**			**−589**	**12**	**14–02**	**−357**	**111**	**1881**	**1380**
4	**11/2/1958**			**−426**	**8**	**04–12**	**−275**	**103**	**1026**	**976**
5	**30/10/2003**			**−383**	**5**	**18–23**	**−258**	**98**	**2147**	**1815**
6	*24/11/2001*			*−221*	*10 F*	*07–17*	*−150*	*93*	*2006*	*1010*
7	*15/5/2005*			*−247*	*5*	*04–09*	*−133*	*171*	*1184*	*994*
8	*25/9/2001*			*−102*	*4*	*22–02*	*−62*	*44*	*1753*	*1433*
9	**06/11/2001**			**−292**	**5**	**02–07**	**−259**	**168**	**1991**	**1675**
10	*15/7/2000*			*−301*	*9 F*	*16–01*	*−171*	*137*	*2023*	*1514*
11	20/11/2003			−422	12 F	09–21	−204	100	1698	1247
12	6/4/2000			−287	6 F	17–23	−152	74	1550	804
13	31/3/2001			−387	5	04–09	−238	148	946	917
14	09/11/2004			−263	23 F	12–11	−173	75	1912	1050
15	7/11/2004			−374	11 F	20–07	−209	70	1491	992
16	11/4/2001			−271	8 F	16–24	−145	58	1699	1262

[a]Listed are the intensity (Dst_{min}), main phase (MP) duration, mean *Dst* during MP (mean Dst_{MP}), maximum *Dst* difference between successive MP hours $(\delta Dst/\delta t)_{MPmax}$, AE_{max}, and mean *AE* during MP (mean AE_{MP}). For the Carrington event, the *H* component of the geomagnetic field is used rather than *Dst*. The letter F in MP duration indicates fluctuating MP. The events are listed in decreasing order of the leading edge velocity (ΔSV) of the corresponding CMEs (Table 2). UT dates (column 2) correspond to main phase onset. The bold, italics, and normal fonts correspond to severe space weather (SvSW) both in the heliosphere and at Earth, SvSW in the heliosphere, and normal space weather (NSW) at Earth and NSW both in the heliosphere and at Earth, respectively; see text.

NASA (http://cdaweb.gsfc.nasa.gov/pre_istp/) are used for the Quebec event. In addition, we use information obtained from the study of ice core samples and space weather literature [e.g., *Tsurutani et al.*, 2003; *Skoug et al.*, 2004; *Webb and Allen*, 2004; *Cliver et al.*, 1990; *Cliver and Svalgaard*, 2004; *Terasawa et al.*, 2005].

The ACE satellite at the L1 point between the Sun and Earth (~220 R_E from the Earth with R_E being Earth radius) provides solar wind velocity and density and IMF components. The wind velocity and density are calculated from the measurements using the SWI (solar wind ion) mode of the SWEPAM (Solar Wind Electron Proton Alpha Monitor) instrument, which collects good quality data every 64 s, with 5% energy resolution around the solar wind peak [e.g., *McComas et al.*, 1998; *Skoug et al.*, 2004]. The SWI mode, however, can fail during energetic particle events at high solar wind speed. At these times, SWEPAM makes measurements at the lowest-energy end of its range (up to 1.3 keV, corresponding to ~500 km/s) and hence does not cover the solar wind distribution. We use these SWI mode failures as one indicator of severe space weather, recognizing that they are only due to energetic particle fluxes. To avoid the possibility of losing data, the SWEPAM instrument also collects 64 s data in another mode called SSTI (search/supra thermal ion) mode, once every ~32 min. The SSTI mode uses nearly the entire sweep energy range (250 eV–17 keV) of SWEPAM with 10–12% energy resolution. We use the SSTI data when there are gaps in SWI data, although the density during the periods of extreme solar wind speed ($>1500\,km\,s^{-1}$) is not used because of large uncertainty [e.g., *Skoug et al.*, 2004]. The ACE data are time shifted to the Earth based on the ACE-Earth distance and solar wind velocity.

Geomagnetic storms are considered as an indicator of space weather. The analysis of *Dst* data gives 83 intense ($Dst_{min} < -100$ nT) storms since 1998. The characteristics of the storms are defined as the following: (1) intensity (Dst_{min}) is the minimum value of *Dst* reached during the main phase (MP), (2) MP duration is the time duration between the main phase onset and Dst_{min}, (3) $\int Dst_{MP}$ is the integrated *Dst* during the MP, (4) mean Dst_{MP} is $\int Dst_{MP}$/MP duration, (5) $(\delta Dst/\delta t)_{MPmax}$ is the maximum difference in *Dst* between successive hours during the MP, and (6) mean AE_{MP} is $\int AE_{MP}$/MP duration (Table 1).

The characteristics at the leading edge of CMEs (or CME fronts) are obtained. The leading edge is considered as when the solar wind velocity (and IMF *B*) increases rapidly; it is found to reach peak values

Table 2. Characteristics at the Leading Edge of the CMEs That Caused Different Types of Space Weather (Listed by Bold, Italics, and Normal Fonts) Since 1998 and the Carrington Event of 1859, the Quebec Event of March 1989, and an Event in February 1958[a]

	No. of UT Date and Time[b]				2 h Mean Values From CME Front							
	D	M	Y	UT	ΔSV (km/s)	SV (km/s)	SD (cm^{-3})	SP (nPa)	B (nT)	B_z (nT)	B_y (nT)	IEF_y (mV/m)	CFP ($\times 10^4$)
1	**1/9/1859**					**no data**							
2	*29/10/2003*			*05:45*	*1145 ± 288*	*1789*	*>15*	*>90*	*23*	*0.78*	*0.48*	*−1.39*	*24.57*
3	**13/3/1989**			-	**840**	**>840**	**15**	**46**			**data gap**		
4	**11/2/1958**			-	**700**	**1100**				**no data**			
5	**30/10/2003**			**17:05**	**609 ± 197**	**1557**	**>15**	**>60**	**34**	**−7.67**	**17.72**	**11.94**	**138.71**
6	*24/11/2001*			*06:07*	*383 ± 39*	*841*	*42*	*61*	*30*	*−4.08*	*8.69*	*3.43*	*0.56*
7	*15/5/2005*			*03:00*	*342 ± 10*	*795*	*22*	*27*	*14*	*0.66*	*3.32*	*−0.52*	*0.04*
8	*25/9/2001*			*20:39*	*301 ± 20*	*675*	*31*	*28*	*20*	*−1.94*	*12.60*	*1.31*	*0.02*
9	**6/11/2001**			**01:04**	**290 ± 13**	**704**	**28**	**27**	**71**	**−62.74**	**14.38**	**44.16**	**28.97**
10	*15/7/2000*			*14:39*	*275 ± 43*	*897*	*11*	*16*	*32*	*4.15*	*3.69*	*−3.72*	*0.32*
11	20/11/2003			08:31	217 ± 25	671	15	16	27	7.12	23.00	−4.60	0.13
12	6/4/2000			16:05	210 ± 12	579	16	11	23	−13.11	14.68	7.54	0.83
13	31/3/2001			01:13	183 ± 68	610	15	12	54	11.04	34.02	−6.70	0.02
14	9/11/2004			11:11	140 ± 36	793	22	27	31	−9.01	5.50	7.14	26.13
15	7/11/2004			18:35	136 ± 57	613	33	26	41	21.70	3.67	−13.30	9.82
16	11/4/2001			13:34	89 ± 29	589	7	5	15	−4.36	−5.81	2.56	0.31

[a]Listed are the mean values of solar wind velocity (SV), density (SD), dynamic pressure (SP), IMF B, IMF B_z, IMF B_y, IEF_y and coupling function CFP for 2 h from the leading edge of the CMEs, and the difference of mean SV 2 h after and 2 h before the leading edge (ΔSV). The events are listed in decreasing order of ΔSV; see text. The bold, italics, and normal fonts correspond to severe space weather (SvSW) both in the heliosphere and at Earth, SvSW in the heliosphere, and normal space weather (NSW) at Earth and NSW both in the heliosphere and at Earth, respectively.

[b]Date and time correspond to the CME front velocity at ACE.

within about 2 h from the start of the rapid increase. The mean values of solar wind velocity (SV), solar wind density (SD), solar wind dynamic pressure (SP), IMF B, IMF B_z, IMF B_y, IEF_y (impressed electric field), and coupling function crystal-field parameter (CFP) for 2 h from the sudden velocity increase (or CME front) are calculated (Table 2). The coupling function CFP is obtained as CF ($= SV^{4/3}B_T^{2/3}\sin^{8/3}(\theta_c/2)$) and CFP ($= CF.SP^{1/2}$), with SV and SP being solar wind velocity and dynamic pressure, and B_T and θ_c being IMF B intensity and clock angle ($\theta_c = \arctan(B_y/B_z)$; CF represents the dayside magnetopause magnetic flux merging rate ($d\Phi/dt$) [*Newell et al.*, 2007]. The empirical function CFP is found to represent a good measure of the efficiency of CME-magnetosphere coupling, although there are a number of such functions. IEF_y ($= V_x \times B_z$) is the east-west component of the interplanetary electric field (positive east) with V_x being the X component of the solar wind velocity (positive toward Earth) and B_z being IMF B_z (positive north). The leading edge velocity (ΔSV) is calculated as the difference between the mean SV 2 h after and 2 h before the leading edge. The ΔSV and SD for the Quebec event on 13 March 1989 (Table 2, number 3) are assumed to be the SV and SD values measured by IMP 8 on 15 March 1989. (The assumption seems qualitatively valid since the ΔSV at the CME front on 13 March would have been much greater than the SV on 15 March. The satellite could make measurements only from 15 March when it came to the solar wind). The ΔSV for the event on 11 February 1958 is inferred from the calculations of *Cliver et al.* [1990]. The date and time of start, peak, and end of the SEP events and their peak intensity are listed in Table 3, with figures in section 4.4.

3. Definition

A severe space weather (SvSW) event in the heliosphere is defined as an event which affected the normal operation of the ACE satellite system (SWI mode of SWEPAM) due to the impact of high-energy charged particles. A SvSW event at the Earth is defined as an event which produced an extreme geomagnetic storm of high mean *Dst* during the main phase (mean $Dst_{MP} < -250$ nT). The known electric power outages happened during some of these SvSW events. The events that did not cause such severe effects are considered normal space weather (NSW). The events are classified based on available data and information. It should be mentioned that all SvSW events might not have been reported and different satellite systems and ground

Table 3. Characteristics of the SEPs Associated With the CMEs That Caused Different Types of Space Weather (Listed by Bold, Italics, and Normal Fonts) Since 1998 and the Carrington Event of 1859, the Quebec Event of 1989, and an Event in February 1958[a]

			UT Date and Time of SEP[b]							
			Peak		End			UT Date and Time of CME Front		
No.	Start D M Y	UT	D	UT	D	UT	SEP Intensity (psu)	D	UT	ΔSV (km/s)
1	1/9/1859			**no data**						
2	*28/10/2003*	*13:00*	*29*	*06:36*	*29*	*14:25*	*5500*	*29*	*05:45*	*1145*
3	13/3/1989	09:50	**data gap**		13	17:35	**data gap**			~840
4	11/2/1958		**no data**							
5	29/10/2003	18:45	30	03:00	31	02:55	869	30	17:05	609
6	*23/11/2001*	*12:35*	*24*	*05:55*	*25*	*00:00*	*1170*	*24*	*06:07*	*383*
7	*13/5/2005*	*18:45*	*15*	*02:40*	*15*	*07:15*	*11*	*15*	*03:00*	*342*
8	*24/9/2001*	*12:05*	*25*	*22:30*	*27*	*13:00*	*1380*	*25*	*20:29*	*301*
9	**4/11/2001**	**16:50**	**06**	**02:20**	**06**	**15:55**	**6870**	**06**	**01:04**	**290**
10	*14/7/2000*	*10:40*	*15*	*09:35*	*15*	*20:10*	*5680*	*15*	*14:39*	*275*
11	20/11/2003	07:55	20	11:30	21	10:20	1	20	08:31	271
12	4/4/2000	16:55	04	20:35	06	21:50	1	06	16:05	210
13	29/3/2001	11:30	29	22:15	31	13:00	4	31	01:13	183
14	9/11/2004	19:30	10	10:05	13	02:40	49	09	11:11	140
15	7/11/2004	18:00	07	23:35	08	17:30	26	07	18:35	136
16	9/4/2001	16:10	10	19:40	12	10:35	14	11	13:34	89

[a]Listed are the date and time of the start, peak, and end of SEPs and their peak intensity at the bow shock. The corresponding date and time of the CME front and the CME front velocity at the L1 point are also listed for easy comparison. The bold, italics, and normal fonts correspond to severe space weather (SvSW) both in the heliosphere and at Earth, SvSW in the heliosphere, and normal space weather (NSW) at Earth and NSW both in the heliosphere and at Earth, respectively; see text.
[b]Date and month correspond to the start of SEP at bow shock.

systems have different tolerance limits and responses, and hence, an event that causes SvSW in one system may not cause SvSW in other systems.

Based on available data, the (known) SvSW events can be distinguished from the NSW events in terms of the characteristics at the leading edge of CMEs. The CMEs having leading edge velocity above a certain threshold alone or together with the associated shocks and SEPs ahead seem to cause SvSW in the heliosphere (at least at ACE), and such CMEs having the IMF B_z also southward at the leading edge cause SvSW at the Earth. Accordingly, there can be three types of space weather events: SvSW in the heliosphere and at Earth, SvSW in the heliosphere and NSW at Earth, and NSW both in the heliosphere and at Earth. The data and literature do not indicate the possibility of NSW in the heliosphere and SvSW at Earth, although high-speed solar wind streams under such conditions can cause continuous injection of a low level of energy into geospace. This, however, is unlikely to cause SvSW on Earth (as defined) because the rate of energy input is low (or not impulsive); however, the energy input can lead to intense geomagnetic storms and long-lived outer radiation belts [e.g., *MacDonald et al.*, 2010; *Liemohn et al.*, 2010].

4. Results

The *Dst* data show two occasions since 1998 (6 November 2001 and 30 October 2003) when extreme geomagnetic storms (mean $Dst_{MP} < -250$ nT) occurred; electric power outages happened during both occasions [e.g., *Pulkkinen et al.*, 2005; *Viljanen et al.*, 2006; *Wik et al.*, 2009; *Marshall et al.*, 2012], and the ACE SWI mode also failed on both occasions. These two events and the Carrington event of 1859, the Quebec event of 1989, and another event in 1958 (mentioned above) are considered as SvSW in both the heliosphere and at Earth (section 4.1). All these events are associated with extreme geomagnetic storms (mean $Dst_{MP} < -250$ nT).

Tables 1–3 list the characteristics of the geomagnetic storms, CMEs, and SEPs associated with the SvSW events in both the heliosphere and at Earth (bold font). The ACE data show five other occasions when the SWI mode failed due to the impact of energetic charged particles at times of high solar wind speed. However, the associated geomagnetic storms were not extreme. These five events (Tables 1–3, *italic*

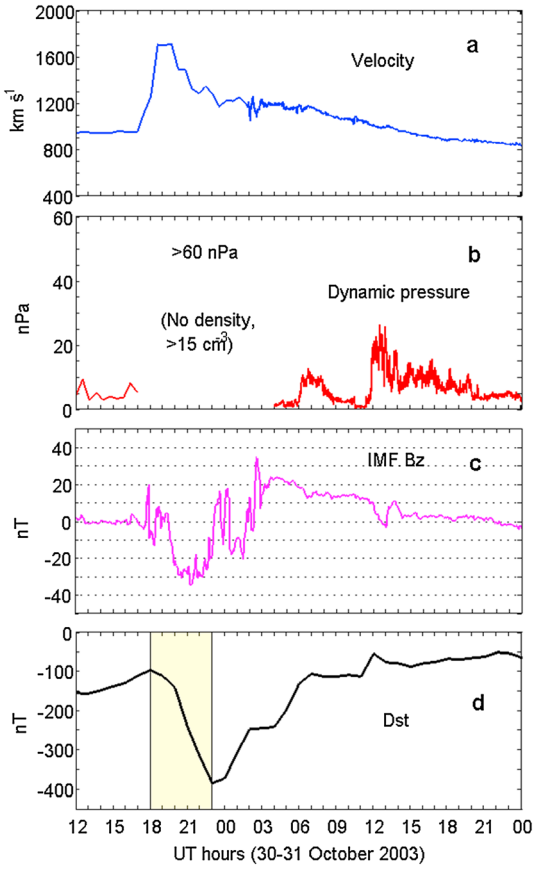

Figure 1. (a) Solar wind velocity, (b) dynamic pressure, (c) IMF B_z, and (d) geomagnetic storm of the space weather event on 30–31 October 2003. The gap in dynamic pressure corresponds to large uncertainty in solar wind density.

font) are considered as SvSW in the heliosphere and NSW at the Earth (section 4.2). The SWI mode is found to fail at the leading edge of the CMEs except in the July 2000 and October 2003 events when the mode failed before the leading edge. There are several other occasions when the ACE solar wind data are not available due to instrument shut off for satellite positioning and meteor showers or low solar wind flux. The characteristics associated with all other super geomagnetic storms ($Dst_{min} < -250$ nT) that occurred since 1998 are also listed (Tables 1–3, normal font) for comparison; they belong to NSW in both the heliosphere and Earth (section 4.3) as they did not seem to affect the operation of the SWI mode in ACE and did not produce extreme geomagnetic storms.

As the data (Tables 1–3) reveal, it is mainly the leading edge velocity (ΔSV) that distinguishes the SvSW and NSW events, and hence, the events are listed in decreasing order of ΔSV. The data also reveal that the intensity of the geomagnetic storms (Dst_{min} and AE_{max}) alone may not indicate the severity of space weather on Earth, although it has traditionally been considered as an indicator. Below, we compare the characteristics of the CMEs with the corresponding space weather effects to understand what determines the severity of space weather. The comparison done with respect to the CME front velocity (shifted to the bow shock nose or otherwise specified) can have some uncertainty in time (within about ±30 min) because the time resolution is 16 s for IMF, 64 s and 32 min for CMEs (from SWI and SSTI), 5 min for SEPs and 1 h for *Dst*, and constant wind velocity is assumed for the time shift. This can slightly change the mean values of the parameters at the CME front but does not seem to affect the conclusions as understood from the standard deviations of all parameters though listed (Table 2) and shown later only for the important parameter ΔSV, for simplicity. All events are not discussed in detail. However, the characteristics of all events (Tables 1–3) seem to agree with the conclusions.

4.1. SvSW in Heliosphere and Earth

The most striking characteristics of the CMEs that caused SvSW in both the heliosphere and at Earth (bold font) are high leading edge velocity ($\Delta SV > 290$ km s^{-1}), high SEP intensity (>850 practical salinity unit (psu) or particle cm^{-2} s^{-1} sr^{-1}), southward IMF B_z, and high mean Dst_{MP} (< -255 nT) (Tables 1–3). The resulting geomagnetic storms (Table 1) also have short duration nonfluctuating MP, large Dst_{min} (< -290 nT) and high $(\delta Dst/\delta t)_{MPmax}$ (>95 nT). All these characteristics together indicate a high amount of energy input to the magnetosphere at a fast rate.

The most famous SvSW event, the Carrington event, occurred on 1 September 1859. The geomagnetic storm of this event obtained from the horizontal component of the geomagnetic field measured at Bombay was shown earlier by *Tsurutani et al.* [2003] and is not repeated here. We discuss its striking characteristics of (1) very short duration (2 h) nonfluctuating MP, very large *H* range (~1710 nT), high mean *H* range (~700 nT), and high $(\delta H/\delta t)_{MPmax}$ (~1390 nT) (Table 1), which are the most extreme in

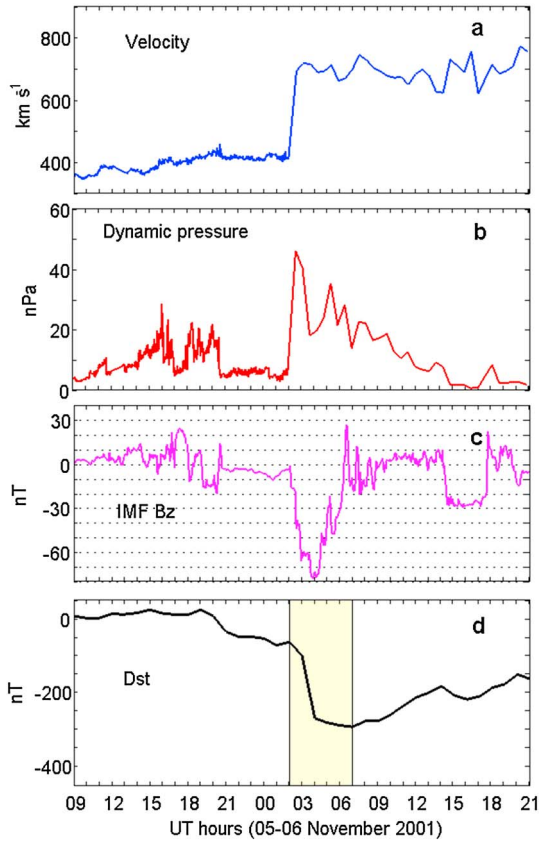

Figure 2. (a) Solar wind velocity, (b) dynamic pressure, (c) IMF B_z, and (d) geomagnetic storm of the space weather events on 5–6 November 2001.

recent history, although they may have some uncertainties. On 1 September 1859, Carrington spotted a cluster of enormous dark spots (sunspots) on the Sun, two patches of intensely bright and white light (solar flare) erupted from the sunspots, 5 min later the fireballs vanished, and within hours, their impacts were felt across the globe [*Carrington*, 1859]. The *impacts* might have been caused by an extreme CME of high impulsive energy (or power), with very high leading edge velocity and IMF B_z southward with no fluctuations for about 2 h from the leading edge. The event caused SvSW (mean H range of ~700 nT). As understood from *Carrington* [1859], the event also caused failure of telegraph communications and occurrence of brilliant auroras. Satellite systems like the ACE SWI mode in the heliosphere if present on the CME path would have been affected. The event might have also caused an intense shower of high-energy protons on the polar atmosphere. The estimate from the concentration of nitrates in ice core samples provides a high-energy (>30 MeV) omnidirectional proton fluence of 18.8×10^9 cm^{-2} for the event, which is twice as big as the estimate for any other event in last 500 years [*Townsend*, 2003].

Cliver and Svalgaard [2004] estimated that the first particles from the Sun arrived at the Earth within a few hours, although the peak intensity of the particle distribution arrived with the shock about 17.6 h later. *Gopalswamy et al.* [2005b] estimated a velocity of ~2380 km s^{-1} for the delay of 17.5 h. *Tsurutani et al.* [2003] studied the geomagnetic storm of the Carrington event. They showed that the Carrington solar flare most likely had an associated intense magnetic cloud ejection, which led to a magnetic storm of intensity ~ −1760 nT, which is in close agreement with the H range measured at Bombay.

Figure 1 shows the CME, IMF B_z, and geomagnetic storm of the Halloween 2003 SvSW event (30–31 October 2003). The solar wind velocity (Figure 1a) obtained using the SWEPAM SSTI mode suddenly increases at ~18:00 UT (shifted to the Earth) on 30 October and reaches ~1710 km s^{-1} in about 2 h; the corresponding density is not used because of large uncertainty. Assuming a moderate density of 15 cm^{-3} as usual in CMEs [e.g., *Terasawa et al.*, 2005], the leading edge has a mean dynamic pressure of >60 nPa, mean velocity of 1557 km s^{-1}, and ΔSV of 609 km s^{-1} (Table 2). The IMF B_z (Figure 1c) is also southward for about 5 h from the leading edge (17:30–23:00 UT), with a mean value of −7.67 nT for the first 2 h (Table 2). The corresponding coupling function has the highest value (~139 units, more than 4 times greater than the next lower value). The SEP intensity, however, is weak (869 psu; Table 3). The energetic CME and southward IMF B_z together seem to inject a high amount of energy at a fast rate into the magnetosphere-ionosphere system mainly through continuous and fast magnetic reconnection [*Dungey*, 1961; *Sonnerup*, 1974; *Deng and Matsumoto*, 2001; *Borovsky et al.*, 2008], which leads to SvSW on Earth including satellite system failure [*Webb and Allen*, 2004], power outage (in Sweden) [e.g., *Pulkkinen et al.*, 2005; *Wik et al.*, 2009], extreme geomagnetic storm (Figure 1d) probably through rapid magnetosphere-ring current and/or ionosphere-ring current coupling [e.g., *Cliver et al.*, 1990; *Yokoyama and Kamide*, 1997], abnormally strong eastward electric field penetration [*Abdu et al.*, 2008], and extreme thermospheric and

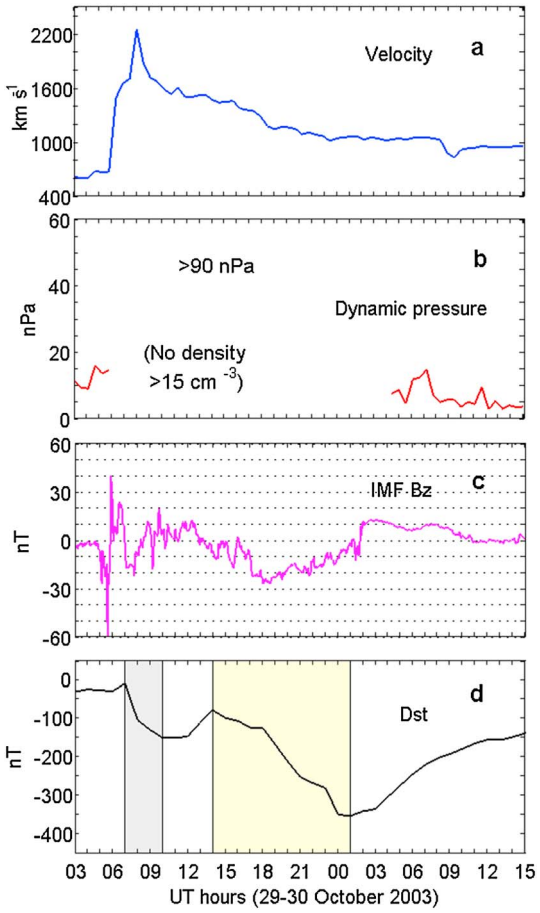

Figure 3. (a) Solar wind velocity, (b) dynamic pressure, (c) IMF B_z, and (d) geomagnetic storm of the space weather events on 29–30 October 2003. The gap in dynamic pressure corresponds to large uncertainty in solar wind density.

ionospheric storms probably through impulsive response [e.g., *Mannucci et al.*, 2005; *Balan et al.*, 2011]. The power outage in Sweden (Malmo event) began at 20:07 UT on 30 October and lasted for 20 to 50 min affecting about 50,000 customers [e.g., *Pulkkinen et al.*, 2005; *Wik et al.*, 2009].

The events on 6 November 2001 (Figure 2) also caused SvSW in the heliosphere and at Earth. At the impact of the CME front, SWEPAM SWI failed and the SSTI velocity (Figure 2a) suddenly increased to 710 km s^{-1} (Table 2) when the density also increased suddenly to 48 cm^{-3}, which gives an impulsive dynamic pressure over 45 nPa (Figure 2b). The IMF B_z also simultaneously becomes largely southward for about 5 h (up to −75 nT). The high CME front velocity (ΔSV = 290 km s^{-1}), high dynamic pressure, and southward IMF B_z together caused SvSW on Earth including an electric power outage in New Zealand [e.g., *Marshall et al.*, 2012] and an extreme geomagnetic storm.

The corresponding SEP event, which started crossing GOES 10 on 4 November and peaked during 5–6 November, seems to be the most intense of all SEPs in this study (Table 3 and section 4.4). But the ACE SWI mode failed only at the impact of the CME front on 6 November at ~02 UT (shifted to bow shock) when the speed suddenly increased and the SEP intensity also sharply peaked (6870 psu), suggesting that the CME front might have accelerated the high-energy charged particles further, which caused the SWI failure. Also, although the SEP intensity and southward IMF B_z on 6 November 2001 were 7 times more intense than those on 30 October 2003, the power outage on 6 November [*Marshall et al.*, 2012] was not as serious as that on 30 October 2003 when the CME front velocity was twice as fast (Table 2), suggesting again that the CME front velocity may be the most important parameter for SvSW.

4.2. SvSW in Heliosphere and NSW on Earth

The five other CMEs that seem to cause SvSW in the heliosphere (failure of SWI in ACE) and NSW at Earth (Tables 1–3, *italics*) also have high leading edge velocity (ΔSV > 275 km s^{-1}), but the IMF B_z is northward at the leading edge. A few events (6 and 8, Table 2), however, have mean IMF B_z slightly southward for the first 2 h, although it is found to be northward for about an hour from the leading edge. The associated SEPs can be strong or weak, with intensity varying by over 500 times (Table 3).

Figure 3 shows the Halloween event of October 2003. The SWI mode was found to fail on 28 October at 12:41 UT at L1 point (~13:10 UT at bow shock) when the wind velocity became high (~810 km s^{-1}) probably due to the shock ahead of the CME; the SEP (Table 3 and section 4.4) also started crossing the L1 point around this time. The low intensity part of the SEP might have been accelerated by the high wind velocity; the combination of the high wind velocity and SEP causes the SWI mode failure. The SSTI velocity on 29 October (Figure 3a) has two sudden increases, one at ~06:00 UT up to 1650 km s^{-1} and other at ~07:30 UT up to

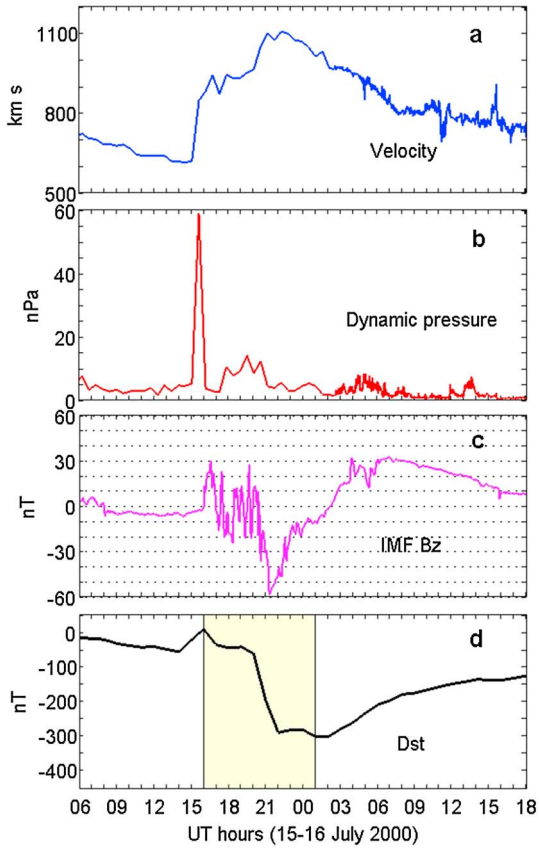

Figure 4. (a) Solar wind velocity, (b) dynamic pressure, (c) IMF B_z, and (d) geomagnetic storm of the space weather event on 15–16 July 2000.

2240 km s^{-1}, which agree with the velocity (~2000 km s^{-1}) obtained from Geotail data [*Terasawa et al.*, 2005]. The corresponding ACE density has large uncertainty. However, as *Terasawa et al.* [2005] calculated from Geotail measurements, the leading edge has density ~15 cm^{-3}. The event has very high leading edge velocity (SV = 1789 km s^{-1} and ΔSV = 1145 km s^{-1}), high dynamic pressure (>90 nPa), and high SEP intensity (Table 3). The IMF B_z (Figure 3c), however, undergoes north-south fluctuations for about 7 h from the leading edge, it is northward at the leading edge, and its mean for the first 2 h is also northward (Table 2). The event could therefore cause only NSW on Earth.

Nevertheless, the IMF B_z turned slightly southward for a short duration between the two velocity impulses (Figures 3a and 3c), which produced a short-duration geomagnetic storm of intensity −151 nT (Figure 3d). Later when the IMF B_z turns southward at around 14 UT, there is no impulse in the velocity. It gradually decreases from ~1500 km s^{-1} to 1000 km s^{-1} during 14–01 UT. That seems to inject low rate of energy into the magnetosphere-ionosphere system through slow magnetic reconnection [e.g., *Kan*, 1988], which results in NSW on Earth. This event with high but gradual velocity variation and southward IMF B_z does not produce SvSW on Earth, stressing the need for an impulsive increase in velocity for SvSW, discussed in section 5.

During the 15 July 2000 event (Figure 4), the SWI mode failed on 14 July at around 11:05 UT at the L1 point (~11:45 UT at bow shock) when the wind velocity was high (~580 km s^{-1}) and an intense SEP started passing the L1 point about an hour earlier (~10:40 at bow shock; Table 3). This again seems to indicate the acceleration of the low intensity part of the SEP by high wind velocity; again, the combination of high wind velocity and SEPs caused the SWI failure. On 15 July, the SSTI wind velocity (Figure 4a) shows an impulsive increase at ~14:40 UT up to 900 km s^{-1} with a ΔSV of 275 km ~ s^{-1}; the proton density (not shown) and hence dynamic pressure (Figure 4b) also increase sharply up to 50 nPa like a spike (Table 2). The IMF B_z, however, undergoes north-south fluctuations with a northward

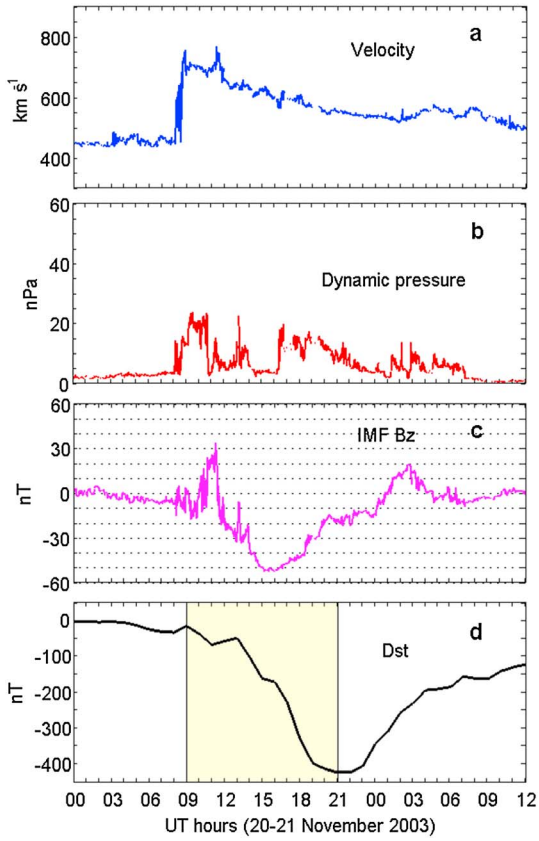

Figure 5. (a) Solar wind velocity, (b) dynamic pressure, (c) IMF B_z, and (d) geomagnetic storm of the space weather event on 20–21 November 2003.

meanof 4.15 nT for the first 2 h (Table 2), which gives a low value for the coupling function (0.323 units). The event therefore could cause only NSW at the Earth. The event on 15 May 2005 has a CME of high leading edge velocity ($\Delta SV = 342\ km\ s^{-1}$), a weak SEP (~11 psu; Table 3), and IMF B_z northward at the leading edge (Table 2), which seem to cause the failure of SWI in ACE (or SvSW in the heliosphere) and NSW at the Earth. The other two events in this category (numbers 6 and 8) also have high CME front velocity ($\Delta SV = 383\ km\ s^{-1}$ and $301\ km\ s^{-1}$), medium SEPs (~1170 psu and 1380 psu), and IMF B_z northward at the CME front, although the mean for the first 2 h is slightly negative.

4.3. NSW in Heliosphere and Earth

As the data reveal, all six events that caused NSW in both the heliosphere and at Earth, although they produced super (but not extreme) geomagnetic storms (Tables 1, 2, numbers 11–16), have low and fluctuating leading edge velocity ($\Delta SV < 220\ km\ s^{-1}$) and north-south fluctuating IMF B_z at the leading edge. However, three of them (numbers 14–16, Table 3) are associated with comparatively intense SEPs (14, 26, and 49 psu) compared to a weak SEP (11 psu) corresponding to SvSW in the heliosphere (number 7), which again seems to indicate the importance of high CME front velocity. A few examples are discussed. On 20 November 2003, the solar wind velocity (Figure 5a) increases up to $750\ km\ s^{-1}$ but with fluctuations, and the associated SEP is very weak (<1 psu). The mean values of SV, ΔSV, and SP for 2 h from the leading edge are also low ($671\ km\ s^{-1}$, $217\ km\ s^{-1}$, and 16 nPa; Table 2). On 7 November 2004, the SEP is comparatively intense (26 psu; Table 3), and the wind velocity (Figure 6a) increases in small steps up to $700\ km\ s^{-1}$ when there is a large rise in SP up to 50 nPa (Figure 6b), mainly due to a large increase in density (not shown). The mean values for 2 h from the leading edge are again small ($SV = 613\ km\ s^{-1}$, $\Delta SV = 136\ km\ s^{-1}$, and SP = 26 nPa; Table 2). Such CMEs with low and fluctuating leading edge velocities do not seem to have enough impulsive energy to cause SvSW in the heliosphere. In addition, the IMF B_z (Figures 5c and 6c) undergoes large north-south fluctuations for several hours from the leading edge, with

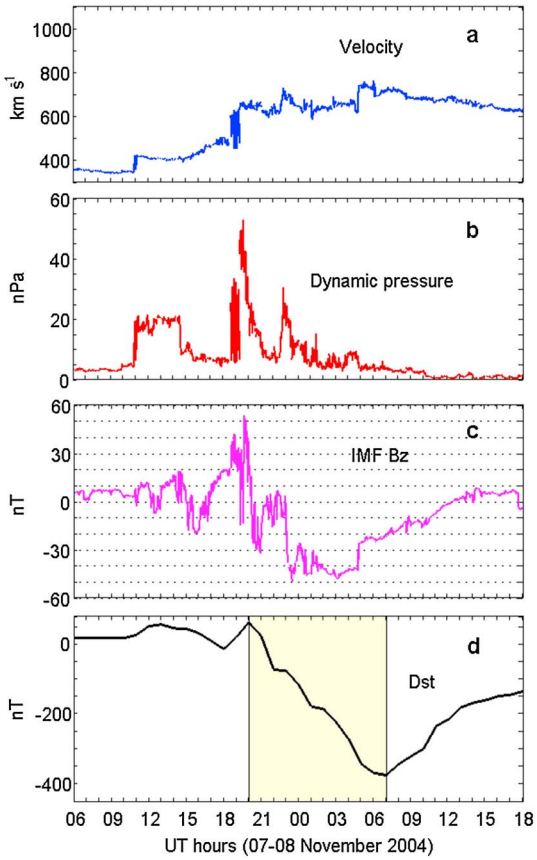

Figure 6. (a) Solar wind velocity, (b) dynamic pressure, (c) IMF B_z, and (d) geomagnetic storm of the space weather event on 07–08 November 2004.

mean values northward (Table 2). The events could therefore inject only a low rate of energy intermittently into the magnetosphere [e.g., *Kan*, 1988], which results in NSW on Earth, including super (but not extreme) geomagnetic storms ($Dst_{min} = -422$ nT and -374 nT) of long-duration fluctuating MPs (Figures 5d and 6d).

The NSW event on 31 March 2001 (Tables 1–2, number 13) is interesting as it produced the strongest geomagnetic storm (short MP and high mean Dst_{MP}) of this category. However, the corresponding SEP is weak (~4 psu); the wind velocity (Figure 7a) has a sudden but small increase up to 650 km s^{-1}, with a mean value of only 610 km s^{-1} ($\Delta SV = 183$ km s^{-1}); and the pressure (Figure 7b) fluctuates up to 50 nPa mainly due to density, with a mean value of 12 nPa for the first 2 h. The IMF B_z (Figure 7c) is northward for about 3 h from the leading edge, with a mean of ~11 nT (Table 2) for the first 2 h, and then becomes southward for about 5 h with minimum fluctuations. This type of CMEs seems to inject a low rate of energy into the magnetosphere for short durations [e.g., *Frey et al.*, 2003], which results in NSW including short-duration (5 h) nonfluctuating super geomagnetic storms (Figure 7d).

Some of the NSW events (Table 1, numbers 11 and 13) have large $(\delta Dst/\delta t)_{MPmax}$ (>100 nT), suggesting that in the long-duration fluctuating MPs, there are short durations when *Dst* decreases rapidly, and these short durations correspond to large southward IMF B_z with no (or minimum) fluctuations. During these periods, the maximum energy available from the CMEs could be injected into the magnetosphere at a fast rate, which in turn could cause stronger than normal space weather on Earth though not severe.

4.4. Solar Energetic Particles

As mentioned in section 1, SEPs and their space weather effects have been studied by several scientists [e.g., *Cliver et al.*, 1990; *Marusek*, 2007; *Singh et al.*, 2010]. In this section, we present the SEP events with energy

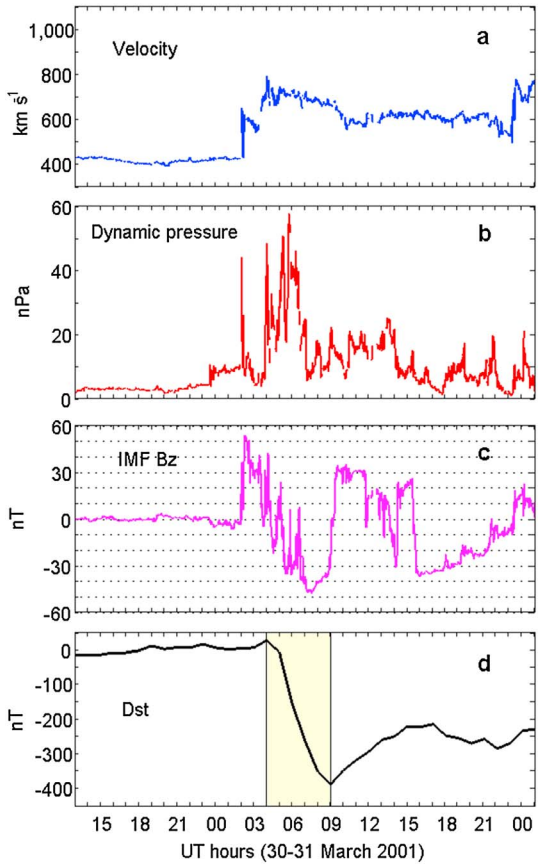

Figure 7. (a) Solar wind velocity, (b) dynamic pressure, (c) IMF B_z, and (d) geomagnetic storm of the space weather event on 30–31 March 2001.

>30 MeV, the effects of which were discussed in sections 4.1. In addition to their characteristics listed in Table 3, Figure 8 shows five SEP events in four panels. Figures 8a and 8b (second event) are for SvSW in both the heliosphere and at Earth, Figures 8b (first event) and 8c are for SvSW in the heliosphere and NSW at Earth, and Figure 8d is for NSW in both the heliosphere and at Earth. The main characteristics of the SEPs and their association with CMEs and space weather are listed.

(1) SEP flux varies gradually and takes ~1.5 to 3 days to cross L1. (2) SEPs arrived at the L1 point before the CME front, and SvSW happened at the L1 point during the passage of the SEPs but at the impact of CME front except in two cases. (3) In two cases (July 2000 and October 2003), SvSW happened at the L1 point before the arrival of CME front when the background wind velocity was high (~810 km s^{-1} and 580 km s^{-1}) probably due to the shocks ahead of the CMEs. (4) The intensity of the SEPs associated with SvSW events varies by over 500 times, and in one case, it is even much weaker than the SEPs associated with three NSW events. (5) Of the two SvSW events at the Earth, the SEP associated with the more severe event (30 October 2003; Figures 1 and 8b) is over 7 times weaker compared to the less severe event (6 November 2001; Figures 2 and 8a), although the CME front, SEP peak, and strong southward IMF B_z all coincided for the weaker SvSW event. (6) In contrast, the CME front velocity of all SvSW events (bold and italics) is greater than that of all NSW events by over 50 km s^{-1}, and the CME front of the more severe SvSW at the Earth is twice as fast compared to the less severe SvSW. These observations seem to indicate that (a) although SEPs are important for SvSW in the heliosphere, they seem to become effective when accelerated by the fast CME front or high background wind due to the shocks ahead and (b) SEPs alone cannot distinguish between all SvSW and NSW events. The observations seem to agree with the suggestion that high-speed CMEs are a necessary condition for the occurrence of SEP events [e.g., *Kahler and Vourlidas*, 2005].

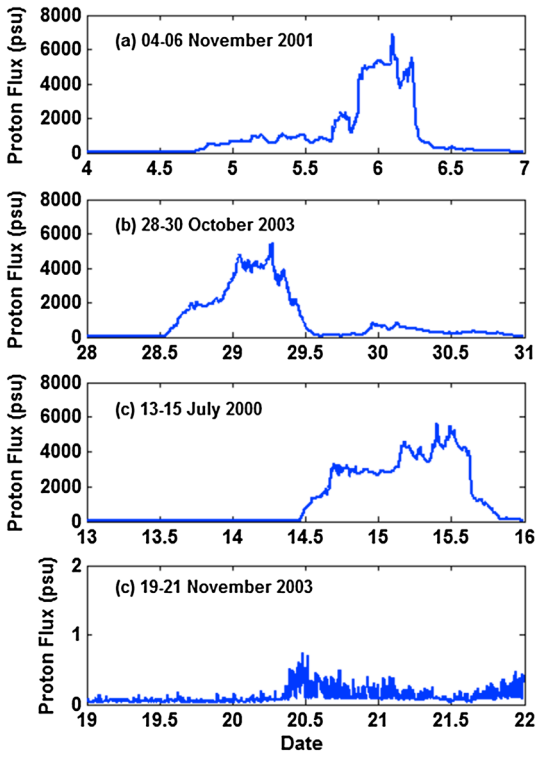

Figure 8. The >30 MeV SEP flux density at bow shock during (a) 4–6 November 2001, (b) 28–30 October 2003, (c) 13–15 July 2000, and (d) 19–21 November 2003 space weather events.

5. Discussion

The results that seem to identify the causes of SvSW are discussed. The characteristics at the leading edge of CMEs (or CME front) seem to determine the severity of space weather. The impulsive energy at the CME front, which is mainly due to the high impulsive velocity and partly due to density, caused SvSW in the heliosphere (failure of SWI in ACE) probably by suddenly accelerating the high-energy particles in the SEPs ahead directly or through the shocks. Based on available data, the minimum impulsive velocity (sudden nonfluctuating increase over the background) required to cause SWI failure in ACE seems over 275 km s^{-1} (Table 2). Such CMEs with the IMF B_z also southward from the leading edge cause SvSW on Earth including extreme geomagnetic storms with mean $Dst_{MP} < -250$ nT; the known electric power outages also happened during some of these SvSW events. The CMEs with low leading edge velocity cause NSW even though the density is high (Figures 5–7). The importance of the leading edge velocity is highlighted in Figure 9 that reproduces the velocity of six CMEs. As shown, the higher the leading edge velocity (ΔSV), the more severe the space weather, like faster weather fronts and tsunami fronts causing more severe damage through impulsive action. Like other physical systems, electronic systems seem affected more severely by impulsive than gradual impacts of charged particles.

The importance of ΔSV and IMF B_z can be appreciated further from Figure 10, which compares the values of ΔSV, SP, IMF B_z, and CFP at the leading edge of all 16 events. The events with ΔSV >275 km s^{-1} caused failure of SWI in ACE (bold and italics), of which the events (bold) with the IMF B_z also southward at the leading edge caused SvSW at the Earth through efficient and impulsive CME-magnetosphere coupling (high CFP). All events (normal font) that have low ΔSV (<220 km s^{-1}) or no ΔSV caused NSW in both the heliosphere and at Earth. Events with very small ΔSV but SV increasing to high values (>750 km s^{-1}) and having high dynamic pressure also cause only NSW as illustrated in Figure 11; this event produced a super geomagnetic storm ($Dst_{min} = -271$ nT) in response to fluctuating IMF B_z. There are several other such cases (e.g., 4 May 1998 and 17–18 September 2000, not included in the tables) when SV increased gradually to over 900 km s^{-1} but caused NSW with large geomagnetic storms ($Dst_{min} < -200$ nT).

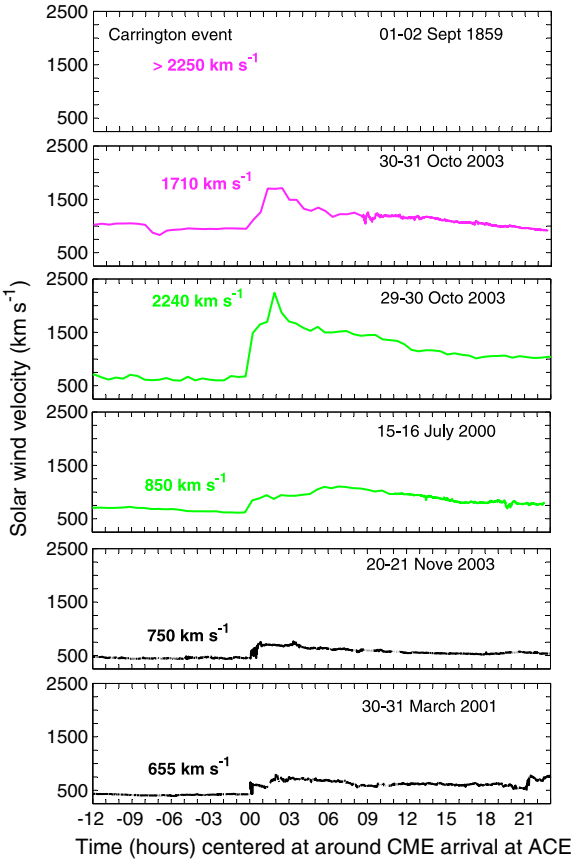

Figure 9. Solar wind velocity of six space weather events on the dates noted. The different colors correspond to the different types of space weather; see text.

A comparison of events seems to clarify the causes of SvSW. The most famous SvSW event [*Carrington*, 1859] might have had the fastest leading edge velocity ΔSV (Figures 9 and 10) and nonfluctuating southward IMF B_z at the leading edge. Although both the Halloween 2003 events (Figures 1 and 3) with high ΔSV caused SvSW in the heliosphere, the one (30–31 October 2003) with IMF B_z also southward at the leading edge caused SvSW at the Earth (Figure 1). As another comparison, while the event on 30–31 October 2003 produced SvSW in both the heliosphere and at Earth, the event on 30–31 March 2001 (Figure 7) with low ΔSV and northward IMF B_z at the leading edge caused only NSW, although both events produced super geomagnetic storms of same intensity (Figures 1d and 7d and Table 1). The strong and weak ionospheric storms observed during these almost identical geomagnetic storms have been a puzzle [*Balan et al.*, 2011] (Figures 2b and 5b), which is understood in terms of the differences in the CME front velocity, orientation of the IMF B_z at the CME front, and mean Dst_{MP}. One has to be careful while considering the intensity of geomagnetic storms as basis for studying ionosphere-thermosphere storms.

Systematic in situ observations of solar wind began in 1962 [*Neugebauer and Snyder*, 1966]. The fastest solar wind speed (>2000 km s^{-1}) prior to the ACE era was recorded on 4 August 1972 [e.g., *Zastenker et al.*, 1978]. *Cliver et al.* [1990] calculated the maximum solar wind speed associated with 23 geomagnetic storms during 1938–1989, which shows speeds over 1000 km s^{-1} for 16 events. However, the time history of the speed and IMF are not available to check how many of them have sudden nonfluctuating increase in speed and IMF B_z southward at the sudden increase. As mentioned in section 1, a highly impulsive CME occurred on 23 July 2012 though was not Earth directed [e.g., *Baker et al.*, 2013; *Russell et al.*, 2013]. The impact of the CME if Earth directed would have been more severe than modeled [*Ngwira et al.*, 2013] if the IMF B_z at the CME front were southward instead of zero/northward.

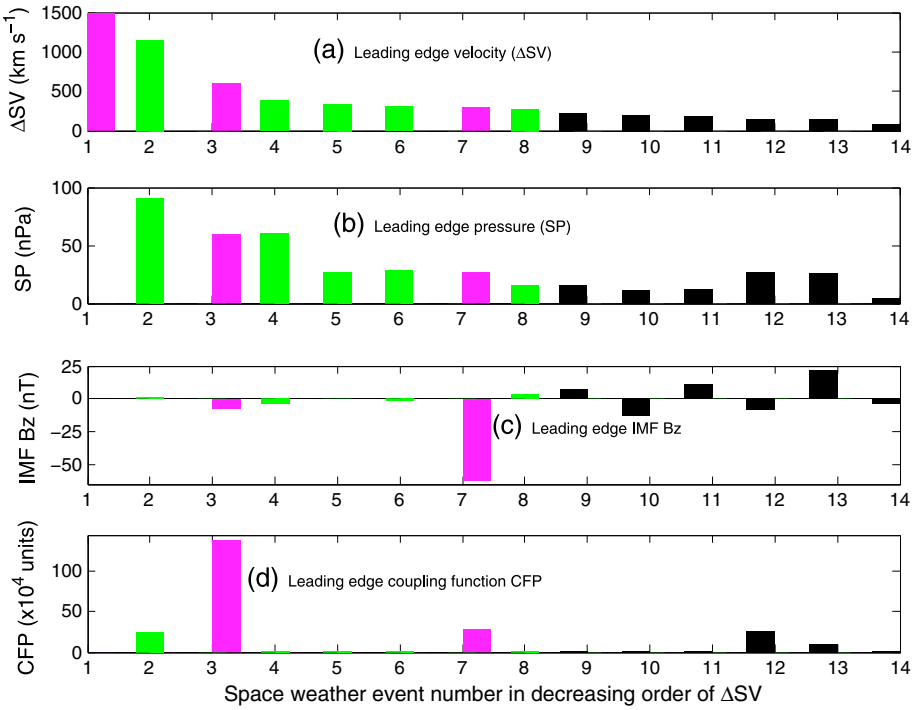

Figure 10. The mean leading edge velocity ΔSV (limited to 1500 km s^{-1} for clarity), dynamic pressure SP, IMF B_z, and coupling function CFP for 2 h from the leading edge of the CMEs corresponding to the 16 major space weather events, arranged in decreasing order of ΔSV (Table 2). The different colors correspond to the different types of space weather; see text.

5.1. Prediction of SvSW

The results indicate that ΔSV, IMF B_z at ΔSV, and mean Dst_{MP} can be used to predict SvSW as illustrated in Figure 12. The events since 1998 are shown by circles. The Carrington and Quebec events are shown by red stars. The possible SvSW event on 11 February 1958 is shown by a black star. No other geomagnetic storm since 1957 is found to have mean $Dst_{MP} < -250$ nT. As shown, all SvSW events in the heliosphere (that caused failure of the SWI mode in ACE) have ΔSV >275 km s^{-1}, and no NSW event has ΔSV >220 km s^{-1}. The sudden nonfluctuating increase of solar wind velocity (ΔSV) by over 275 km s^{-1} may therefore indicate SvSW in the heliosphere. All SvSW events at the Earth have mean $Dst_{MP} < -255$ nT along with ΔSV >285 km s^{-1} and IMF B_z simultaneously southward. All other events have mean $Dst_{MP} > -240$ nT. The geomagnetic storms of mean Dst_{MP} less than this threshold (< -250 nT) may therefore indicate SvSW at the Earth, especially when the MP is of short duration. The mean AE_{MP} (Table 1) is also a good indicator of SvSW at the Earth since 1990 (but not before), maybe because the quality of the *AE* data before 1990 is different from that since 1990 (M. Nose, Kyoto WDC, private communication).

6. Conclusions

It has been known that severe space weather (SvSW) can cause extensive social and economic disruptions in the high-technology society. It is therefore important to understand what determines the severity of space weather and whether it can be predicted. An analysis of the solar-geophysical data indicates that (1) it is the impulsive energy and orientation of the IMF B_z at the leading edge of the CMEs (or CME front) that determine the severity of space weather. (2) The CMEs having high impulsive leading edge velocity (sudden nonfluctuating increase by over 275 km s^{-1} over the background) caused severe space weather (SvSW) in the heliosphere, either directly or through the shocks and SEPs ahead. (3) Such CMEs which also show the IMF B_z southward from the leading edge caused SvSW at the Earth including extreme geomagnetic storms of mean $Dst_{MP} < -250$ nT during main phases. The known electric power outages happened during

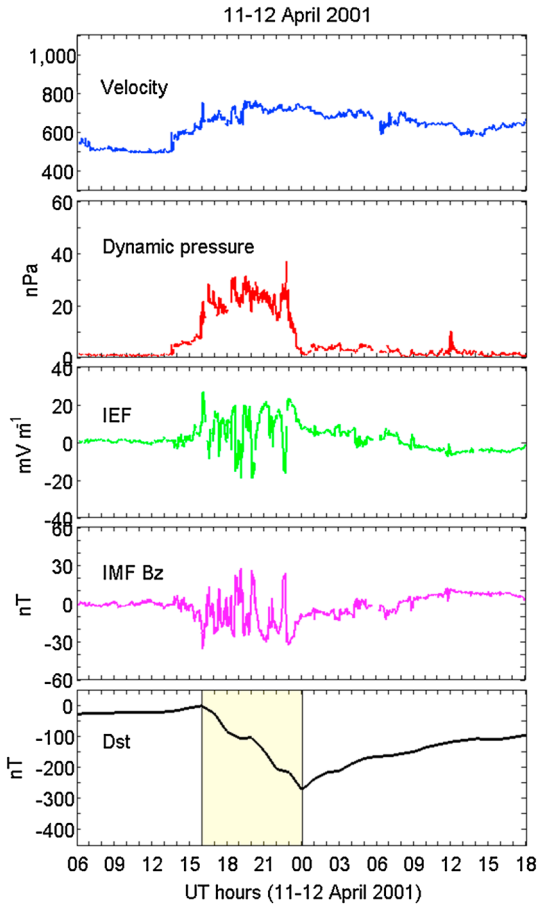

Figure 11. (a) Solar wind velocity, (b) dynamic pressure, (c) IMF B_z, and (d) geomagnetic storm of the space weather event on 11–12 April 2001.

some of these SvSW events. (4) The higher the impulsive velocity, the more severe the space weather through impulsive action. Measurements of the velocity and density of CMEs as close to the Sun as possible and the orientation of IMF B_z at the CME front can be used for predicting/forecasting SvSW, and mean Dst_{MP} of geomagnetic storms can be used for checking SvSW events.

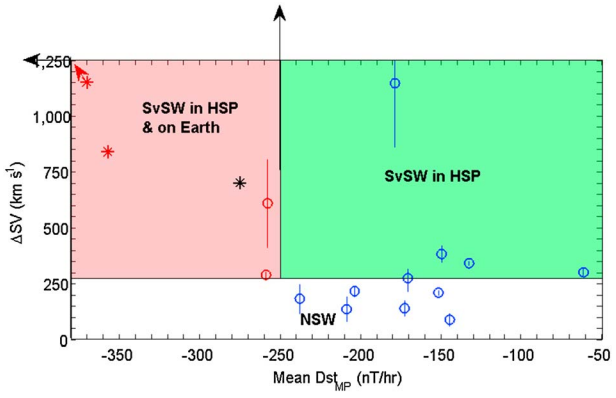

Figure 12. Scatterplots showing the relationship between the CME front velocity ΔSV and the mean Dst_{MP}. The white, green, and red color regions correspond to the different types of space weather. The circles correspond to the events since 1998; the red stars are for the Carrington event and Quebec event, and the black star is for a possible SvSW event on 11 February 1958; see text.

Acknowledgments

We thank the ACE, GOES, and IMP science and engineering teams, Kyoto World Data team, and authors of the excellent space weather literature for the data and information used. The CME and IMF data are obtained using ACE (http://www.srl.caltech.edu/ACE/ASC/) and IMP (http://cdaweb.gsfc.nasa.gov/pre_istp/) satellites; SEP data used are obtained using GOES satellite (http://cdaweb.gsfc.nasa.gov/cgi-bin/eval2.cgi) (OMNI_HRO_5MIN), and *Dst* and *AE* data are obtained from Kyoto WDC (http://wdc.kugi.kyoto-u.ac.jp/dstdir/). We also thank A. Viljanen for the reprints and discussion and the referees for critical comments and good suggestions. N. Balan thanks Nagoya University and National Cheng Kung University for Visiting Professor Positions. The work of Tulasi Ram is partially supported by the Department of Science and Technology (India) under the project GITA/DST/TWN/P-47/2013. Work at Los Alamos was performed under the auspices of the U.S. Department of Energy, with support from the NASA ACE program. This work was supported by Grants-in-Aid for Scientific Research (25247080) from the Japan Society for the Promotion of Science.

Michael Liemohn thanks Yihua Zheng and another reviewer for their assistance in evaluating this paper.

References

Abdu, M. A., et al. (2008), Abnormal evening vertical plasma drift and effects on ESF and EIA over Brazil-South Atlantic sector during the 30 October 2003 superstorm, *J. Geophys. Res.*, *113*, A07313, doi:10.1029/2007JA012844.

Baker, D. N. (2002), How to cope with space weather, *Science*, *297*, 1486–1487.

Baker, D. N., X. Li, A. Pulkkinen, C. M. Ngwira, M. L. Mays, A. B. Galvin, and K. D. C. Simunac (2013), A major solar eruptive event in July 2012: Defining extreme space weather scenarios, *Space Weather*, *11*, 1–7, doi:10.1002/swe.20097.

Balan, N., H. Alleyne, S. Walker, H. Reme, I. McCrea, and A. Aylward (2008), Magnetosphere-ionosphere coupling during the CME events of 07–12 November 2004, *J. Atmos. Sol. Terr. Phys.*, doi:10.1016/j.jastp.2008.03.015.

Balan, N., K. Shiokawa, Y. Otsuka, T. Kikuchi, D. Vijaya Lekshmi, S. Kawamura, M. Yamamoto, and G. J. Bailey (2010), A Physical mechanism of positive ionospheric storms at low and mid latitudes through observations and modeling, *J. Geophys. Res.*, *115*, A02304, doi:10.1029/2009JA014515.

Balan, N., M. Yamamoto, J. Y. Liu, Y. Otsuak, H. Liu and H. Luhr (2011), New aspects of thermospheric and ionospheric storms revealed by CHAMP, *A Most Popular Papers*, *J. Geophys. Res.*, *116*, A07305, doi:10.1029/2010JA0160399.

Barbieri, L. P., and R. E. Mahmot (2004), October-November 2003' space weather and operations lessons learned, *Space Weather*, *2*, S09002, doi:10.1029/2004SW000064.

Barnard, L., M. Lockwood, M. A. Hapgood, M. J. Owens, C. J. Davis, and F. Steinhilber (2011), Predicting space climate change, *Geophys. Res. Lett.*, *38*, L16103, doi:10.1029/2011GL048489.

Batista, I. S., E. R. de Paula, M. A. Abdu, N. B. Trivedi, and M. E. Greenspan (1991), Ionospheric effects of the March 13, 1989, magnetic storm at low and equatorial latitudes, *J. Geophys. Res.*, *96*(13), 943–13,952.

Batista, I. S., M. A. Abdu, J. R. Souza, F. Bertoni, M. T. Matsuoka, P. O. Camargo, and G. J. Bailey (2006), Unusual early morning development of the equatorial anomaly in the Brazilian sector during the Halloween magnetic storm, *J. Geophys. Res.*, *111*, A05307, doi:10.1029/2005JA011428.

Benz, A. O. (2008), Flare Observations, *Living Rev. Sol. Phys.*, *5*, 1.

Bolduc, L. (2002), GIC observations and studies in the Hydro-Québec power system, *J. Atmos. Sol. Terr. Phys.*, *64*, 1793–1802, doi:10.1016/S1364-6826(02)00128-1.

Borovsky, J. E., M. Hesse, J. Birn, and M. M. Kuzentsova (2008), What determines the reconnection rate at the dayside magnetosphere?, *J. Geophys. Res.*, *113*, A07210, doi:10.1029/2007JA012645.

Carrington, R. C. (1859), Description of a singular appearance seen in the Sun on September 1, 1859, *Mon. Not. R. Astron. Soc.*, *20*, 13–15.

Cliver, E. W., and L. Svalgaard (2004), The 1989 solar terrestrial distrubances and current limits of extreme space weather activity, *Sol. Phys.*, *224*, 407.

Cliver, E. W., J. Feynman, and H. B. Garrett (1990), An estimate of the maximum speed of the solar wind, 1938–1989, *J. Geophys. Res.*, *95*, 17,103–17,112, doi:10.1029/JA095iA10p17103.

Deng, X. H., and H. Matsumoto (2001), Rapid magnetic reconnection in the Earth's magnetosphere mediated by whistler waves, *Nature*, *410*, 557–560, doi:10.1038/35069018.

Dungey, J. W. (1961), Interplanetary magnetic field and the auroral zones, *Phys. Rev. Lett.*, *6*, 47–48.

Ebihara, Y., et al. (2005), Ring current and the magnetosphere-ionosphere coupling during the super storm of 20 November 2003, *J. Geophys. Res.*, *110*, A09S22, doi:10.1029/2004JA010924.

Frey, H. U., T. D. Phan, S. A. Fuselier, and S. B. Mende (2003), Continuous magnetic reconnection at Earth' magnetopause, *Nature*, *426*(6966), 533–537, doi:10.1038/nature02084.

Fuller-Rowell, T. J., M. V. Codrescu, R. J. Moffett, and S. Quegan (1994), Response of the thermosphere and ionosphere to geomagnetic storms, *J. Geophys. Res.*, *99*, 3893, doi:10.1029/93JA02015.

Gonzalez, W. D., J. A. Joselyn, Y. Kamide, H. W. Kroehl, G. Rostoker, B. T. Tsurutani, and V. M. Vasyliunas (1994), What is a geomagnetic storm?, *J. Geophys. Res.*, *99*, 5771, doi:10.1029/93JA02867.

Gopalswamy, N., S. Yashiro, G. Michalek, H. Xie, R. P. Lepping, and R. A. Howard (2005a), Solar source of the largest geomagnetic storm of cycle 23, *Geophys. Res. Lett.*, *32*, L12S09, doi:10.1029/2004GL021639.

Gopalswamy, N., L. Barbieri, G. Lu, S. P. Plunkett, and R. M. Skoug (2005b), Introduction to the special section: Violent Sun-Earth connection events of October-November 2003, *Geophys. Res. Lett.*, *32*, L03S01, doi:10.1029/2005GL022348.

Hapgood, M. A. (2011), Towards a scientific understanding of the risk from extreme space weather, *Adv. Space Res.*, *47*, 2059–2072, doi:10.1016/j.asr.2010.02.007.

Heelis, R. A., J. J. Sojka, M. David, and R. W. Schunk (2009), Storm time density enhancements in the mid latitude dayside ionosphere, *J. Geophys. Res.*, *114*, A03315, doi:10.1029/2008JA013690.

Huang, C. M., M. Q. Chen, and J. Y. Liu (2010), Ionospheric positive storm phases at the magnetic equator close to sunset, *J. Geophys. Res.*, *115*, A07315, doi:10.1029/2009JA014936.

Kahler, S. W., and A. Vourlidas (2005), Fast coronal mass ejection environments and the production of solar energetic particle events, *J. Geophys. Res.*, *110*, A12S01, doi:10.1029/2005JA011073.

Kamide, Y., N. Yokoyama, W. Gonzalez, B. T. Tsurutani, I. A. Daglis, A. Brekke, and S. Masuda (1998a), Two-step development of geomagnetic storms, *J. Geophys. Res.*, *103*, 6917–6921, doi:10.1029/97JA03337.

Kamide, Y., et al. (1998b), Current understanding of magnetic storms: Storm-substorm relationships, *J. Geophys. Res.*, *103*(A8), 17,705–17,728, doi:10.1029/98JA01426.

Kan, J. R. (1988), A theory of patchy and intermittent reconnections for magnetospheric flux transfer events, *J. Geophys. Res.*, *93*, 5613–5623, doi:10.1029/JA093iA06p05613.

Kappenman, J. G. (1996), Geomagnetic storms and their impact on power systems, *IEEE Power Eng. Rev.*, *16*, 5–8.

Kelley, M. C., J. J. Makela, J. L. Chau, and M. J. Nicolls (2003), Penetration of the solar wind electric field into the magnetosphere/ionosphere system, *Geophys. Res. Lett.*, *30*(4), 1158, doi:10.1029/2002GL016321.

Kikuchi, T., T. Araki, H. Maeda, and K. Maekawa (1978), Transmission of polar electric fields to the equator, *Nature*, *273*, 650–651.

Lanzerotti, L. J. (2001), Space weather effects on technologies, in *Space Weather*, edited by P. Song, H. J. Singer, and G. L. Siscoe, 11 pp., AGU, Washington, D. C.

Liemohn, M., W. M. Jazowski, J. U. Kozyra, N. Ganushkina, M. F. Thomsen, and J. E. Borovsky (2010), CIR versus CME drivers of the ring current during intense magnetic storms, *Proc. R. Soc. A*, *466*, 3305–3328, doi:10.1098/rspa.2010.0075.

Lin, C. H., A. D. Richmond, R. A. Heelis, G. J. Bailey, G. Lu, J. Y. Liu, H. C. Yeh, and S. Y. Su (2005), Theoretical study of the low and mid latitude ionospheric electron density enhancement during the October 2003 storm: Relative importance of the neutral wind and the electric field, *J. Geophys. Res.*, *110*, A12312, doi:10.1029/2005JA011304.

Lu, G., L. P. Goncharenko, M. J. Nicolls, A. I. Maute, A. J. Coster, and L. J. Paxton (2012), Ionospheric and thermospheric variations associated with prompt penetration electric, *J. Geophys. Res.*, *117*, A08312, doi:10.1029/2012JA017769.
MacDonald, E. A., L. W. Blum, P. S. Gary, M. F. Thomsen, and M. H. Denton (2010), High-speed stream driven inferences of global wave distributions at geosynchronous orbit: Relevance to radiation-belt dynamics, *Proc. R. Soc. A*, *466*, 3351–3362, doi:10.1098/rspa.2010.0076.
MacQueen, R. M., et al. (1974), The outer solar corona as observed from skylab: Preliminary Results, *Astrophys. J.*, *187*, L85–L88.
Mannucci, A. J., B. T. Tsurutani, B. A. Iijima, A. Komjathy, A. Saito, W. D. Gonzalez, F. L. Guarnieri, J. U. Kozyra, and R. Skoug (2005), Dayside global ionospheric response to the major interplanetary events of October 29–30, 2003 "Halloween Storms", *Geophys. Res. Lett.*, *32*, L12S02, doi:10.1029/2004GL021467.
Manoharan, P. K. (2006), Evolution of coronal mass ejections in the inner heliosphere: A study using white-light and scintillation images, *Sol. Phys.*, *235*, 345–368.
Marshall, R. A., M. Dalzell, C. L. Waters, P. Goldthorpe, and E. A. Smith1 (2012), Geomagnetically induced currents in the New Zealand power network, *Space Weather*, *10*, S08003, doi:10.1029/2012SW000806.
Marusek, J. A. (2007), Solar storm threat analysis. *Impact 1–29*. [Available at http://www.breadandbutterscience.com/SSTA.]
Matuura, N. (1972), Theoretical models of ionospheric storms, *Space Sci. Rev.*, *13*, 124–189.
Mayr, H. G., and H. Volland (1973), Magnetic storm characteristics of the thermosphere, *J. Geophys. Res.*, *78*, 2251, doi:10.1029/JA078i013p02251.
McComas, D. J., S. J. Bame, P. Barker, W. C. Feldman, J. L. Phillips, and P. Riley (1998), Solar wind electron proton alpha monitor (SWEPAM) for the advanced composition explorer, *Space Sci. Rev.*, *86*, 563–612.
McKenna-Lawlor, S. M. P. (2008), Predicted interplanetary shocks/particles at Mars compared with in-situ observations: An overview, *Planet. Space Sci.*, *56*, 1703–1712.
Medford, L. V., L. J. Lanzerotti, J. S. Kraus, and C. J. Maclennan (1989), Transatlantic earth potential variations during the March 1989 magnetic storms, *Geophys. Res. Lett.*, *16*(10), 1145–1148, doi:10.1029/GL016i010p01145.
Neugebauer, M., and C. W. Snyder (1966), Mariner 2 observations of the solar wind, 1, Average properties, *J. Geophys. Res.*, *71*, 4469, doi:10.1029/JZ071i019p04469.
Newell, P. T., T. Sotirelis, K. Liou, C.-I. Meng, and F. J. Rich (2007), A nearly universal solar wind-magnetosphere coupling function inferred from 10 magnetospheric state variables, *J. Geophys. Res.*, *112*, A01206, doi:10.1029/2006JA012015.
Ngwira, C. M., et al. (2013), Simulation of the 23 July 2012 extreme space weather event: What if this extremely rare CME was Earth directed?, *Space Weather*, *11*, 671–679, doi:10.1002/2013SW000990.
Prolss, G. W. (1995), Ionospheric F region storms, in *Handbook of Atmospheric Electrodynamics*, edited by H. Volland, pp. 195–248, CRC Press, Boca Raton, Fla.
Pulkkinen, A., S. Lindahl, A. Viljanen, and R. Pirjola (2005), Geomagnetic storm of 29–31 October 2003: Geomagnetically induced currents and their relation to problems in the Swedish high-voltage power transmission system, *Space Weather*, *3*, S08C03, doi:10.1029/2004SW000123.
Pulkkinen, T. (2007), Space weather: Terrestrial prespective, *Living Rev Sol Phys*, *4*, 1.
Rastogi, R. G. (1977), Geomagnetic storms and electric fields in the equatorial ionosphere, *Nature*, *268*, 422.
Reames, D. V., L. M. Barbier, and C. K. Ng (1996), The spatial distribution of particles accelerated by coronal mass ejection—Driven shocks, *Astrophys. J.*, *466*, 473–486, doi:10.1086/177525.
Riley, P. (2012), On the probability of occurrence of extreme space weather events, *Space Weather*, *10*, S02012, doi:10.1029/2011SW000734.
Russell, C. T., X. W. Zhou, P. J. Chi, H. Kawano, T. E. Moore, W. K. Peterson, J. B. Cladis, and H. J. Singer (1999), Sudden compression of the outer magnetosphere associated with an ionospheric mass ejection, *Geophys. Res. Lett.*, *26*, 2343, doi:10.1029/1999GL900455.
Russell, C. T., et al. (2013), The very unusual interplanetary coronal mass ejection of 2012 July 23: A blast wave mediated by solar energetic particles, *Astrophys. J.*, *770*, 38, doi:10.1088/0004-637X/770/1/38.
Schwenn, R. (2006), Space weather: The solar prespective, *Living Rev. Sol. Phys.*, *3*, 2.
Shea, M. A., D. F. Smart, K. G. McCracken, G. A. M. Dreschhoff, and H. E. Spence (2006), Solar proton events for 450 years: The Carrington event in perspective, *Adv. Space Res.*, *38*, 232–238, doi:10.1016/jasr.2005.02.100.
Shibata, K., and T. Magara (2011), Solar Flares: Magnetohydrodynamic processes, *Living Rev. Sol. Phys.*, *8*, 6.
Singh, A. K., D. Siingh, and R. P. Singh (2010), Space weather: Physics, effects and predictability, *Surv. Geophys.*, *31*, 581–638, doi:10.1007/s10712-010-9103-1.
Skoug, R. M., J. T. Gosling, J. T. Steinberg, D. J. McComas, C. W. Smith, N. F. Ness, Q. Hu, and L. F. Burlaga (2004), Extremely high speed solar wind: 29–30 October 2003, *J. Geophys. Res.*, *109*, A09102, doi:10.1029/2004JA010494.
Sojka, J. J., M. Davis, R. W. Schunk, and R. A. Heelis (2012), A modelling study of the longitudinal dependence of storm time midlatitude dayside total electron content enhancements, *J. Geophys. Res.*, *117*, A02315, doi:10.1029/2011JA017000.
Sonnerup, B. U. O. (1974), Magnetopause reconnection rate, *J. Geophys. Res.*, *79*, 1546, doi:10.1029/JA079i010p01546.
Terasawa, T., et al. (2005), Determination of shock parameters for the very fats interplanetary shock on 29 October 2003, *J. Geophys. Res.*, *110*, A09S12, doi:10.1029/2004JA010941.
Townsend, L. W. (2003), Carrington flare of 1850 as a prototypical worst-case solar energetic particle event, *IEEE Trans Nucl Sci.*, *50*(6), 2307–2309.
Tsurutani, B. T., W. D. Gonzalez, G. S. Lakhina, and S. Alex (2003), The extreme magnetic storm of 1–2 September 1859, *J. Geophys. Res.*, *108*(A7), 1268–1275, doi:10.1029/2002JA009504.
Tulasi Ram, S., C. H. Liu, and S.-Y. Su (2010), Periodic solar wind forcing due to recurrent Coronal holes during 1996–2009 and its impact on Earth's geomagnetic and ionospheric properties during extreme solar minimum, *J. Geophys. Res.*, *115*, A12340, doi:10.1029/2010JA015800.
Tulasi Ram, S., N. Balan, B. Veenadhari, S. Gurubaran, S. Ravindran, T. Tsugawa, H. Liu, K. Niranjan, and T. Nagatsuma (2012), First observational evidence for opposite zonal electric fields in equatorial E and F region altitudes during a geomagnetic storm period, *J. Geophys. Res.*, *117*, A09318, doi:10.1029/2012JA018045.
Viljanen, A., A. Pulkkinen, R. Pirjola, K. Pajunpaa, P. Posio, and A. Koistinen (2006), Recordings of geomagnetically induced currents and a nowcasting service of the Finnish natural gas pipe line system, *Space Weather*, *4*, S10004, doi:10.1029/2006SW000234.
Webb, D. F., and J. H. Allen (2004), Spacecraft and ground anomalies related to the October-November 2003 solar activity, *Space Weather*, *2*, S03008, doi:10.1029/2004SW000075.
Wik, M., R. Pirjola, H. Lundstedt, A. Viljanen, P. Wintoft, and A. Pulkkinen (2009), Space weather events in July 1982 and October 2003 and the effects of geomagnetically induced currents on Swedish technical systems, *Ann. Geophys.*, *27*, 1775–1787.
Yokoyama, N., and Y. Kamide (1997), Statistical nature of geomagnetic storms, *J. Geophys. Res.*, *102*, 14,215–14,222, doi:10.1029/97JA00903.
Zastenker, G. N., V. V. Temny, C. d'Uston, and J. M. Bosqued (1978), The form and energy of the shock waves from the solar flares of August 2, 4, and 7, 1972, *J. Geophys. Res.*, *83*, 1035, doi:10.1029/JA083iA03p01035.